Signaling-dependent immobilization of acylated proteins in the inner monolayer of the plasma membrane

Elaine F. Corbett-Nelson,[1] David Mason,[1,2] John G. Marshall,[1] Yves Collette,[3] and Sergio Grinstein[1,2]

[1]Division of Cell Biology, The Hospital for Sick Children, Toronto, M5G 1X8, Canada
[2]Department of Biochemistry, University of Toronto, Toronto, M5S 1A8, Canada
[3]Institut de Cancérologie de Marseille, UMR 599 Institut National de la Santé et de la Recherche Médicale, 13009 Marseille, France

Phospholipids play a critical role in the recruitment and activation of several adaptors and effectors during phagocytosis. Changes in lipid metabolism during phagocytosis are restricted to the phagocytic cup, the area of the plasmalemma lining the target particle. It is unclear how specific lipids and lipid-associated molecules are prevented from diffusing away from the cup during the course of phagocytosis, a process that often requires several minutes. We studied the mobility of lipid-associated proteins at the phagocytic cup by measuring fluorescence recovery after photobleaching. Lipid-anchored (diacylated) fluorescent proteins were freely mobile in the unstimulated membrane, but their mobility was severely restricted at sites of phagocytosis. Only probes anchored to the inner monolayer displayed reduced mobility, whereas those attached to the outer monolayer were unaffected. The immobilization persisted after depletion of plasmalemmal cholesterol, ruling out a role of conventional "rafts." Corralling of the probes by the actin cytoskeleton was similarly discounted. Instead, the change in mobility required activation of tyrosine kinases. We suggest that signaling-dependent recruitment of adaptors and effectors with lipid binding domains generates an annulus of lipids with restricted mobility.

Introduction

Elimination of pathogens by phagocytosis is an essential component of the innate immune response. Phagocytosis is a complex sequence of signaling and cytoskeletal remodeling events that culminates in the engulfment of microorganisms into a vacuole. The process is initiated by recognition of ligands on the surface of the pathogen by specialized phagocytic receptors. Progressive zippering of receptors to multiple ligands on the target particle drives the apposition of the host cell membrane to the surface of the pathogen. In this specialized area of contact, known as the phagosomal cup, receptor clustering unleashes a signaling cascade that ultimately promotes actin polymerization, pseudopod extension, and particle internalization.

Phosphoinositides play a critical role in the initiation of phagocytosis. Phosphatidylinositol-4,5-bisphosphate (PtdIns[4,5]P_2) undergoes a biphasic change at the phagocytic cup: an initial, transient increase that is followed by its virtual disappearance by the time phagosomal sealing is complete (Botelho et al., 2000). These changes appear to be essential for successful completion of phagocytosis, as interference with PtdIns(4,5)P_2 biosynthesis or catabolism impairs particle engulfment (Azzoni et al., 1992; Liao et al., 1992; Araki et al., 1996; Cox et al., 1999). Conversion to phosphatidylinositol-3,4,5-trisphosphate (PtdIns[3,4,5]P_3) is partly responsible for the disappearance of PtdIns(4,5)P_2 from the phagosomal cup. Accordingly, formation of PtdIns(3,4,5)P_3 can be readily detected at the base of the nascent phagosome (Marshall et al., 2001), and inhibition of phosphatidylinositol-3-kinases, which are responsible for its synthesis, effectively blocks the uptake of phagocytic particles that are >3 μm (Cox et al., 1999). Remarkably, the reported changes in PtdIns(4,5)P_2 and PtdIns(3,4,5)P_3 are confined to the phagocytic cup, without detectable alteration of the inositides in the unengaged (bulk) plasma membrane (PM).

Biological membranes are generally regarded as fluid mosaics wherein lipids or clustered lipid microdomains can diffuse freely (Galbiati et al., 2001). At physiological temperatures,

E.F. Corbett-Nelson and D. Mason contributed equally to this paper.

Correspondence to Sergio Grinstein: sga@sickkids.ca

Abbreviations used in this paper: BODIYP, boron dipyrromethene difluoride; DIC, differential interference contrast; GPI, glycosylphosphatidylinositol; LAT, linker for activation of T cells; LSM, laser-scanning microscopy; MβCD, methyl-β-cyclodextrin; MF, mobile fraction; NBD, nitrobenzoxadiazole; PH, pleckstrin homology; PM, plasma membrane.

The online version of this article contains supplemental material.

The Journal of Cell Biology, Vol. 174, No. 2, July 17, 2006 255–265
http://www.jcb.org/cgi/doi/10.1083/jcb.200605044

such unrestricted lateral diffusion would result in rapid redistribution and homogenization of phospholipids. It is therefore unclear how gradients of inositides can be sustained for the time required for phagosome formation, which can exceed 3–4 min for large particles. Two possibilities can be envisaged: first, the lipids may be continuously generated at sites of phagocytosis and, although able to diffuse, they may be rapidly hydrolyzed as they leave the cup. Thus, a dynamic steady-state gradient could be achieved. Alternatively, the diffusion of lipids at sites of phagocytosis may be restricted, differing from their mobility in the bulk of the plasmalemma. Mobility may be restricted within or across the boundary of the phagocytic cup.

Lipids are important determinants of the distribution of membrane proteins. Extrinsic proteins can associate with lipid headgroups, and transmembrane proteins segregate into microdomains according to the nature of the surrounding lipids. Several important signal transduction proteins associate with membranes by inserting their acyl and prenyl moieties into the hydrophobic domain of the bilayer. It can be anticipated that changes in the lipidic composition of the membrane during phagocytosis would have important consequences on the distribution and hence the activity of signaling proteins. In fact, phosphoinositides are thought to contribute to signal transduction by recruiting adaptor and effector proteins to sites of phagocytosis (Stauffer and Meyer, 1997; Hinchliffe et al., 1998; Oancea et al., 1998; Varnai et al., 1999; Botelho et al., 2000).

Clearly, the distribution and mobility of lipids and lipid-associated proteins is critical for vectorial transduction of signals during phagocytosis. However, the mobility of specific lipids in native membranes is difficult to analyze. Introduction of fluorescent moieties can alter the size, charge, and/or conformation of their headgroup or tail, and defined labeled lipids are rapidly converted to other chemical species. An alternative method frequently used to study lipids in cells, namely, the expression of fluorescent chimeric proteins containing specific lipid binding domains, is of limited use to study mobility. The limitation stems from the fact that the complex formed between the lipid and the chimera is in rapid dynamic equilibrium, with dissociation occurring much faster than the movement of the lipid in the plane of the membrane (Marshall et al., 2001). Because of these limitations and because of their importance in signal transduction, we decided to analyze instead the mobility of lipid-linked proteins at the phagosomal cup. FRAP was used for this purpose. Various constructs were used that targeted either the inner or outer monolayer of the plasmalemma and that resided preferentially or, alternatively, were excluded from areas rich in saturated lipids. Using large phagocytic targets and a combination of bright-field and confocal fluorescence microscopy, we were able to establish that the mobility of saturated lipids is drastically reduced at the phagocytic cup by a process that requires receptor-induced tyrosine phosphorylation.

Results

Mobility of PM-GFP in resting cells

The mobility of membrane-associated molecules in activated macrophages was studied earlier by sedimentation of suspended cells onto IgG-coated surfaces (Marshall et al., 2001). This system has distinct optical advantages, as the membrane becomes activated at a fixed, predictable focal plane. However, this model of abortive phagocytosis does not recapitulate all aspects of the engulfment process and may involve components of cell spreading onto the substratum. On the other hand, phagocytosis of small particles is not amenable to the study of lipid mobility because of the rapidity of the internalization event and the small cup size (Fig. S1, available at http://www.jcb.org/cgi/content/full/jcb.200605044/DC1). As an alternative, we used large (8.3-μm diameter) particles as phagocytic targets. The size of these particles is similar to that of apoptotic cells that are commonly ingested by macrophages (Fadok et al., 1992).

The distribution of PM-GFP in macrophages is shown in Fig. 1. PM-GFP is a chimeric construct of the N-terminal 10 amino acids from Lyn with GFP. The N-terminal sequence of

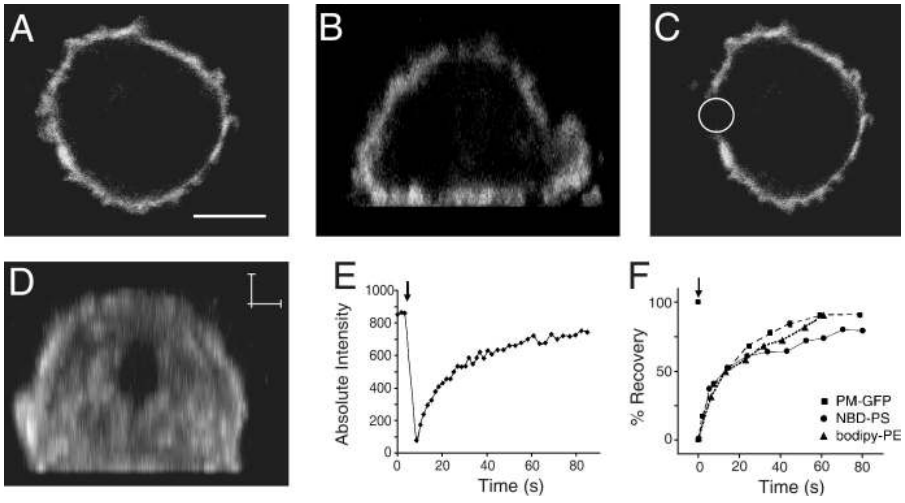

Figure 1. **Distribution and photobleaching of PM-GFP in macrophages.** RAW264.7 cells were transfected with PM-GFP and analyzed by confocal laser-scanning microscopy. (A) Transverse (x vs. y) optical slice acquired near the middle of an otherwise untreated cell. Bar, 5 μm. (B) Sagittal (x vs. z) reconstruction. (C) Transverse slice of the same cell after photobleaching of the area indicated by the circle. (D) Three-dimensional rendering of the photobleached cell. Note that only the front (bleached) half of the cell is illustrated, to facilitate visualization of the bleached area. Bars, 2 μm. Images in A–D are representative of >20 experiments. (E) Course of FRAP. An absolute intensity trace showing a typical bleach of ∼90% is illustrated. (F) Normalized recovery after photobleaching. Shown are recovery of PM-GFP, BODIPY-labeled phosphatidylethanolamine (PE), and NBD-labeled phosphatidylserine (PS). Bleaching was performed at the arrow. Data are means ± SEM of eight individual experiments. Where absent, error bars were smaller than the symbol.

Lyn directs myristoylation and palmitoylation of the chimera, which targets the fluorescent protein to the inner monolayer of the plasmalemma (Teruel et al., 1999). Transverse (x vs. y; Fig. 1 A) and sagittal (x vs. z; Fig. 1 B) sections of the cells confirm that PM-GFP is largely plasmalemmal, although varying amounts of endomembrane staining can be seen, depending on the expression level. The mobility of PM-GFP was initially assessed by FRAP in unstimulated cells. As shown in Fig. 1 C and particularly in the three-dimensional reconstruction of Fig. 1 D, the optical setup used bleached a nearly circular area of ~2 μm in diameter within 1–2 s. Under the conditions of our experiments, ~10–20% of the original intensity remained after bleaching (Fig. 1 E). In otherwise untreated cells, the fluorescence recovered almost completely (Fig. 1 F, squares; and Table I); in eight determinations, the mobile fraction (MF) averaged 1.10 ± 0.04 (these and all subsequent data are presented as means ± 1 SEM of the indicated number of determinations). Recovery was half maximal ($t_{1/2}$) after 15 ± 2 s, indicative of a diffusion coefficient of 1.5×10^{-10} cm^2/s. This value is very similar to that we find for phospholipids in these cells. As shown in Fig. 1 F and Table I, fluorescently labeled phosphatidylserine and phosphatidylethanolamine recover from photobleaching with comparable kinetics, yielding diffusion coefficients 2.4×10^{-10} and 2.2×10^{-10} cm^2/s, respectively. Together, these findings imply that the mobility of PM-GFP in the membrane is limited by association of its acyl chains with other constituents of the bilayer and not by drag imposed by the GFP itself. Accordingly, the diffusion coefficient of free GFP in the cytosol has been estimated at $2.5 - 3.0 \times 10^{-7}$ cm^2/s (Swaminathan et al., 1996), much faster than that of the diacylated construct.

Mobility of PM-GFP at the phagocytic cup

RAW cells were exposed to IgG-opsonized latex beads to assess the mobility of PM-GFP at the phagocytic cup (Fig. 2). The considerable time required for complete engulfment of the large beads (≥6 min; Fig. S1) enabled us to perform photobleaching and measure the recovery of fluorescence before phagocytosis was completed. Fig. 2 (A–C) shows that the area of the membrane engaged in particle recognition and engulfment (the cup) was readily identifiable and sufficiently large to accommodate the ~2-μm bleaching zone that was used. To normalize the recovery for changes in focal plane, photobleaching, or de novo delivery of probe, recovery was also measured at an area of unengaged membrane of the same cell. Although theoretically the MF cannot exceed 100%, membrane convolution at sites of ingestion can occasionally cause the MF to exceed this value. Typical results are shown in Fig. 2 D. Although the unengaged area of the membrane behaved as described for the membrane of resting cells (MF = 0.8–1), the fraction of mobile PM-GFP at the cup was markedly decreased (MF = 0.36 ± 0.01; $n = 8$). The diffusion rate of the remaining MF was indistinguishable from the PM-GFP in the bulk membrane. These findings suggest that the mobility of acylated proteins is diminished in the vicinity of the Fcγ receptors associated with and activated by the phagocytic particle.

Phagosomes undergo membrane remodeling after sealing, a consequence of active fusion and fission events (Vieira et al., 2002). We found that for large beads such as those used in the present study, remodeling starts even before phagocytosis is completed (Fig. S2, available at http://www.jcb.org/cgi/content/full/jcb.200605044/DC1). It was therefore important to ascertain that the failure of PM-GFP fluorescence to recover was a reflection of immobility and not its removal from the membrane. To this end, we performed careful quantitation of the rate of disappearance of PM-GFP and of another membrane marker, glycosylphosphatidylinositol (GPI)-anchored YFP during phagocytosis of large beads. Up to 40% of the fluorescence is lost from the base of the cup in 3 min (Fig. S2). We therefore limited our FRAP experiments to the initial 100 s, when the loss by remodeling is modest.

Mobility of other GFP constructs anchored to the inner monolayer

Stimulatory Fcγ receptors bearing an immunoreceptor tyrosine-based activation motif associate with and become phosphorylated by Src-family kinases, including Lyn. Because the N-terminal sequence used to target PM-GFP to the membrane was derived from Lyn, we considered the possibility that a specific, direct interaction with the receptor complex might account for the reduced mobility of the fluorescent probe. As an alternative strategy to target GFP to the inner aspect of the PM, we attached the C-terminal 9 amino acids of H-Ras to GFP. In addition to

Table I. **Summary of FRAP results at the unengaged PM versus phagosomal cup**

	PM			Phagosomal cup		
Fluorescent moiety	**Recovery**	**$t_{1/2}$ for recovery**	**R^2**	**Recovery**	**$t_{1/2}$ for recovery**	**R^2**
	%			%		
PM-GFP	110	15	0.995	36	8	0.990
PM-GFP + MβCD	127	23	0.996	44	10	0.988
PM-GFP + PP1	96	12	0.996	76	10	0.988
H-Ras-GFP	78	10	0.998	35	4	0.995
K-Ras-GFP	113	9	0.997	90	8	0.992
LAT-GFP	96	6	0.995	99	6	0.997
GPI-YFP	97	8	0.994	99	7	0.987
GPI-YFP + PP1	93	6	0.995	85	8	0.995
PS-NBD	75	9	0.980	—	—	—
PE-BODIPY	93	10	0.975	—	—	—

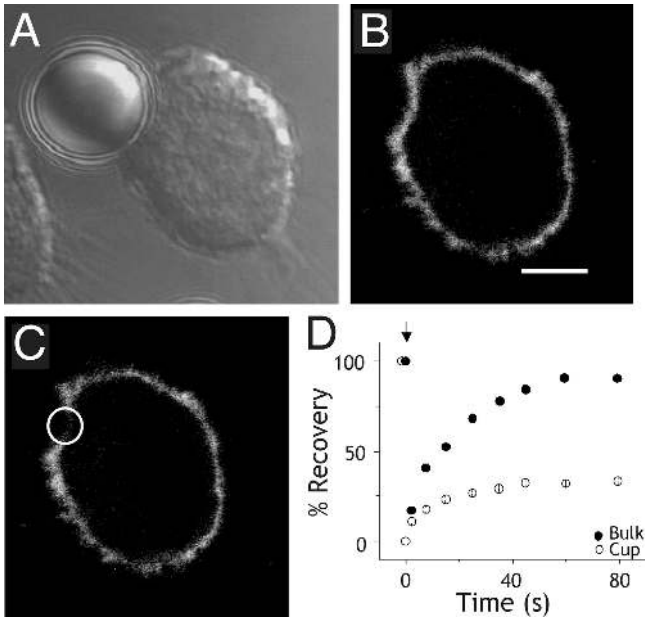

Figure 2. **Photobleaching of PM-GFP at the phagosomal cup.** RAW264.7 cells were transfected with PM-GFP, and phagocytosis was initiated by addition of IgG-opsonized beads (8.3-μm diameter) while the cells were being analyzed by differential interference contrast (DIC) and LSM. (A) DIC image. (B) Corresponding LSM transverse optical slice acquired before bleaching near the middle of the phagocytic cup. Bar, 5 μm. (C) LSM transverse optical slice acquired shortly after bleaching the area indicated by the circle. (D) Course of FRAP. Bleaching was performed at the arrow. Two areas were bleached: one near the middle of the cup (open circles) and the other in an unengaged, contralateral area of the cell membrane (closed circles). Data are means ± SEM of eight individual experiments. Where absent, error bars were smaller than the symbol.

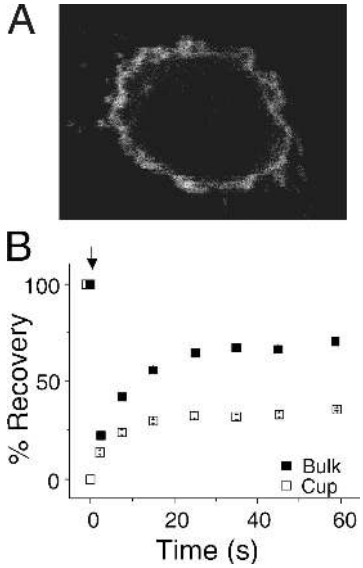

Figure 3. **Photobleaching of GFP-tH.** RAW264.7 cells were transfected with GFP-tH, and phagocytosis was initiated by addition of IgG-opsonized beads while the cells were being analyzed by DIC and LSM. (A) Confocal LSM image taken before bleaching, showing the distribution of GFP-tH. (B) Time course of FRAP of GFP-tH; bleaching was performed at the arrow. Two areas of the cell were bleached: one near the middle of the cup (open squares) and the other in an unengaged, contralateral area of the cell membrane (closed squares). Data in B are means ± SEM of eight individual experiments. Where absent, error bars were smaller than the symbol.

the prenylation that is characteristic of all Ras isoforms, the C terminus of H-Ras is doubly acylated, and the chimeric GFP comprising the 9 amino acids of H-Ras (GFP-tH) undergoes the same posttranslational modifications (Apolloni et al., 2000). As a result, GFP-tH targets almost exclusively to the plasmalemma in BHK cells (Apolloni et al., 2000), as well as in RAW macrophages (Fig. 3 A). As shown in Fig. 3 B (solid squares) and Table I, when photobleached in resting macrophages or in the unengaged region of cells engulfing beads, GFP-tH recovered rapidly ($t_{1/2}$ = 10 ± 0.5 s; n = 8) and extensively (MF = 0.78 ± 0.01). In contrast, at the phagosomal cup, a sizable fraction of GFP-tH was immobile during the period analyzed (MF = 0.37 ± 0.01; n = 8). The diffusion of the MF was similar to that of the unengaged control membrane (Table I). Therefore, two different acylated GFP probes displayed reduced mobility in nascent phagosomes. Because the C terminus of H-Ras is not anticipated to interact with Fc receptors, it is unlikely that direct association with the receptor complex is responsible for the immobilization of either probe.

Role of the actin cytoskeleton in lipid mobility in nascent phagosomes

The preceding data indicate that two different probes anchored to the cytosolic aspect of the membrane exhibit reduced mobility at sites of phagosome formation. One possible obstacle to the movement of inner membrane–associated GFP is the actin cytoskeleton. Accumulation of actin and other cytoskeletal proteins is a well-established feature of phagosome generation (Tse et al., 2003). We therefore considered whether the partial immobilization of PM-GFP and GFP-tH at the cup resulted from steric hindrance by actin-associated proteins. It has been shown that preventing actin polymerization with cytochalasin D does not abrogate bead engagement or the subsequent tyrosine phosphorylation of Fc receptors (Greenberg et al., 1994). In accordance with these findings, we found that when large opsonized beads were added to cytochalasin-treated cells, cup formation was evident (Fig. 4, A and B), enabling us to perform FRAP with minimal actin polymerization. In cells treated with cytochalasin D, the mobility of PM-GFP in the bulk membrane was unaffected (MF = 0.84; Table I). However, the area of the membrane engaged in phagocytosis still showed reduced mobility (Fig. 4 C). To further study this phenomenon, we took advantage of the observation that under normal conditions actin dissociates from the membrane as the phagosome seals. The accumulation of F-actin at the base of the cup and its dissociation from the membrane of recently formed phagosomes is documented dynamically in Video 1 (available at http://www.jcb.org/cgi/content/full/jcb.200605044/DC1). Note that the amount of residual F-actin associated with formed phagosomes is minute, much lower than that of the unengaged PM. Because of the premature membrane remodeling observed during engulfment of large beads, smaller particles (3.1 μm) were used to ensure sufficient retention of the probe in sealed phagosomes (Fig. 4 E). We were thus able to compare the lateral mobility of PM-GFP in actin-depleted sealed phagosomal and PMs. As shown in Fig. 4 F, the MF of the probe in the sealed vacuole

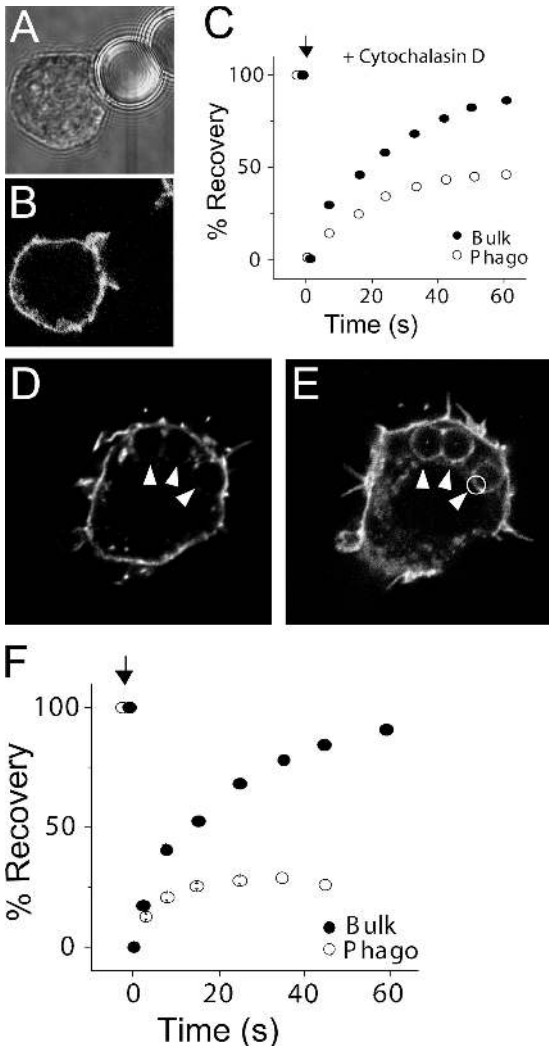

Figure 4. **Role of actin on the MF of PM-GFP in early and formed phagosomes.** (A and B) DIC and LSM images of PM-GFP, respectively, showing the extent of development of phagocytic cups in RAW cells treated with cytochalasin D. Phagocytosis was initiated by the addition of IgG-opsonized beads (8.3-μm diameter). (C) Recovery of PM-GFP fluorescence after photobleaching performed at the cup and an unengaged area of the membrane. (D–F) Photobleaching of PM-GFP in formed phagosomes. Phagocytosis was initiated by addition of IgG-opsonized latex beads (3.1-μm diameter), and after 6 min the cells were fixed and stained with labeled phalloidin to visualize F-actin by LSM (D). (E) Fluorescence of PM-GFP in the same cell stained for actin in D. Arrowheads in D and E indicate the location of three internalized beads. A typical area designated for bleaching is indicated by the circle. (F) Course of FRAP. Bleaching was performed at the arrow. Two areas of each cell were bleached: one in the phagosomal membrane (phago) and the other in the cell membrane (bulk). Data are means ± SEM of seven individual experiments. Error bars were smaller than the symbol.

remained considerably lower than that of the bulk plasmalemma (MF = 0.26 ± 0.02 and 0.9 ± 0.02, respectively; $n = 8$). Qualitatively similar results were obtained using 8.3-μm beads, but the results were less reliable because of the small amount of fluorescence remaining after sealing (unpublished data). Given the small amount of actin that remains associated with the formed phagosome, it is unlikely that the reduced mobility of lipid-associated probes is attributable to physical hindrance by the cytoskeleton.

Mobility of GFP constructs anchored to the outer monolayer

Lipids containing saturated acyl chains are thought to localize preferentially in sphingolipid and cholesterol-enriched microdomains often called "rafts" (Simons and Ikonen, 1997). Cross-linked Fcγ receptors are thought to cluster in similar microdomains (Kwiatkowska and Sobota, 2001). It therefore seemed likely that the reduced mobility of PM-GFP and GFP-tH could result from trapping in poorly mobile raft aggregates at the phagocytic cup. To test this hypothesis, we measured the lateral mobility of GPI-GFP and -YFP, as GPI-linked proteins partition selectively in rafts (Nichols, 2003). When expressed in macrophages, GPI-GFP is present largely in the plasmalemma (Fig. 5 A). That the protein is anchored to the outer monolayer was verified by its accessibility to anti-GFP antibodies added extracellularly to intact cells (unpublished data). Most of the GPI-anchored probe was mobile in resting cells (MF = 0.81 ± 0.04; $n = 8$) and in the unengaged regions of the membrane of cells performing phagocytosis (Table I). The diffusion rate was similar to that of PM-GFP (Fig. 5 D). More important, the MF and rate of diffusion of GPI-GFP or -YFP were virtually identical at the phagocytic cup and elsewhere in the unengaged membrane (Table I). Therefore, the behavior of GPI-anchored probes is distinctly different from that of PM-GFP and GFP-tH.

Role of microdomains in lipid mobility at the cup

It has recently become apparent that different types of lipid microdomains (rafts) can coexist in cells (Kusumi et al., 2004). Therefore, the differential behavior of GPI- and PM-GFP does not necessarily rule out raft involvement in reducing the mobility of PM-GFP. To further explore the role of lipid microdomains, we transfected cells with a lipid-anchored construct that is largely excluded from the rafts. GFP-tK was constructed by adding the C-terminal 17 residues of K-Ras to GFP. This portion of the hypervariable domain of K-Ras includes the prenylation CAAX box plus a polycationic sequence that directs the resulting chimera to anionic lipids of the cytosolic face of the plasmalemma (Apolloni et al., 2000). As anticipated, GFP-tK was predominantly found at the cell membrane (unpublished data). In unstimulated cells, as well as in unengaged regions of the membrane of cells performing phagocytosis, GFP-tK was highly mobile (Table I; MF = 1.13 ± 0.03; $t_{1/2} = 9 \pm 1$ s; $n = 6$). Its mobility was only marginally lower at the phagocytic cup (MF = 0.90 ± 0.03; $t_{1/2} = 7.8 \pm 1.4$ s; $n = 6$). The differential behavior of the various lipid-associated proteins tested suggests that individual microdomains have distinct mobility within nascent phagosomes.

To further test the role of lipid microdomains, we used methyl-β-cyclodextrin (MβCD) to remove cholesterol from the membrane (Klein et al., 1995). Cholesterol is essential for the formation of most lipid rafts, and its removal consistently leads to their destabilization (Kwiatkowska et al., 2003). Treatment of RAW cells with MβCD as described in Materials and methods resulted in sizable removal of plasmalemmal cholesterol, which could be readily visualized by staining the cells with filipin (Fig. 6, A and B). The total cellular content of cholesterol,

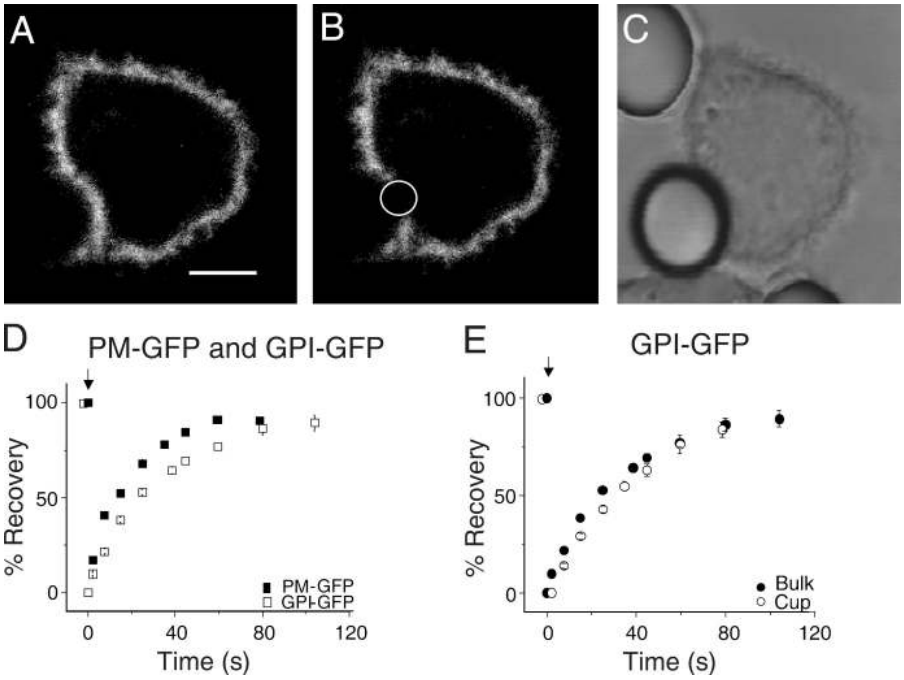

Figure 5. **Photobleaching of GPI-GFP at the phagosomal cup.** RAW264.7 cells were transfected with GPI-GFP, and phagocytosis was initiated by addition of IgG-opsonized beads (8.3-μm diameter) while the cells were being analyzed by differential interference contrast (DIC) and LSM. (A) LSM transverse optical slice acquired before bleaching near the middle of the phagocytic cup. Bar, 5 μm. (B) LSM transverse optical slice acquired shortly after bleaching the area indicated by the circle. (C) Corresponding DIC image. (D) Comparison of the course of FRAP in otherwise unstimulated cells transfected with either GPI- or PM-GFP. (E) Comparison of the course of FRAP of GPI-GFP at the cup (open circles) and in an unengaged region of the PM (closed circles). In D and E, bleaching was performed at the arrow and data are means ± SEM of eight experiments of each type. Where absent, error bars were smaller than the symbol.

determined using a cholesterol oxidase-based spectroscopic assay, was reduced by 50% after treatment with MβCD. Of note, extraction of cholesterol did not affect the mobility of PM-GFP in otherwise untreated cells. The MF (1.27 ± 0.1; $n = 7$) and the diffusion rate ($t_{1/2} = 23 \pm 4$ s) were altered only marginally by pretreatment with MβCD (Fig. 6 D and Table I).

Cholesterol depletion had no discernible effect on the ability of RAW cells to ingest opsonized beads, consistent with earlier findings (Peyron et al., 2000); note, however, that inhibitory effects of MβCD on some types of phagocytosis have also been reported (Peyron et al., 2000; Kwiatkowska and Sobota, 2001). More important, the immobilization of a large fraction of PM-GFP at the phagocytic cup persisted in cholesterol-depleted cells (Fig. 6, C and E; MF = 0.44 ± 0.02; $n = 7$). These findings imply that normal cholesterol content is not essential for the preservation of the microdomains that experience reduced mobility at sites of phagocytosis.

Further evidence that sphingolipid and cholesterol-rich microdomains do not mediate the immobilization of diacylated proteins was obtained by studying the behavior of LAT (linker for activation of T cells). This adaptor is a transmembrane protein known to associate preferentially with such microdomains. As shown in Fig. 6 F, GFP-tagged LAT localized to the PM, as reported for the native protein and for the fluorescent chimera in lymphoid cells (Bonello et al., 2004). Of note, the mobility of LAT at the phagocytic cup was not different from that measured elsewhere in the cell (Fig. 6 G and Table I). These observations suggest that cholesterol-enriched rafts are not noticeably immobilized in the vicinity of engaged Fcγ receptors.

Tyrosine phosphorylation is required to reduce lipid mobility

We next investigated whether the alteration in the mobility of lipid-associated proteins during phagocytosis is a passive consequence of receptor clustering at the cup or requires active signaling. Tyrosine phosphorylation of the Fcγ receptors by Src-family kinases is one of the earliest events in the signaling cascade and is essential for progression of phagocytosis. Inhibition of Src-family kinases with inhibitors such as PP1 and PP2 precludes particle internalization (Majeed et al., 2001; Song et al., 2004), yet does not prevent receptor–ligand association and formation of a well-defined phagocytic cup (Fig. S3, B and E, available at http://www.jcb.org/cgi/content/full/jcb.200605044/DC1). We were therefore able to assess the mobility of both PM-GFP and GPI-YFP at the cup of PP1-inhibited cells. The effectiveness of the kinase inhibitor was verified by its ability to prevent the PLC-mediated hydrolysis of PtdIns(4,5)P_2 (measured using a specific pleckstrin homology [PH] domain; Fig. S3, B and E), a tyrosine phosphorylation–dependent event, and by the virtually complete inhibition of particle engulfment despite the formation of stable incipient cups. As illustrated in Fig. 7, the mobility of the lipid-associated probe was only marginally reduced at the cup, compared with the bulk, unengaged membrane. In eight experiments using PM-GFP, the MF was 0.76 ± 0.03 in the former and 0.96 ± 0.03 in the latter. Similarly, the fraction and half-time of GPI-YFP recovery in the presence of PP1 were not significantly altered (Fig. 7 and Table I).

The possible role of phosphatidylinositol 3-kinase in controlling lipid mobility was also investigated. We initially confirmed that under the conditions used, the inhibitor LY294002 impaired phosphatidylinositol 3-kinase activity, as it prevented the accumulation of 3′-phosphorylated polyphosphoinositides normally observed at the cup during the early stages of phagocytosis (Fig. S3, C and F). As reported earlier (Araki et al., 1996; Cox et al., 1999), treatment with inhibitors of this kinase arrested the development of phagosomes at an intermediate stage, where cup formation is evident but sealing is impaired,

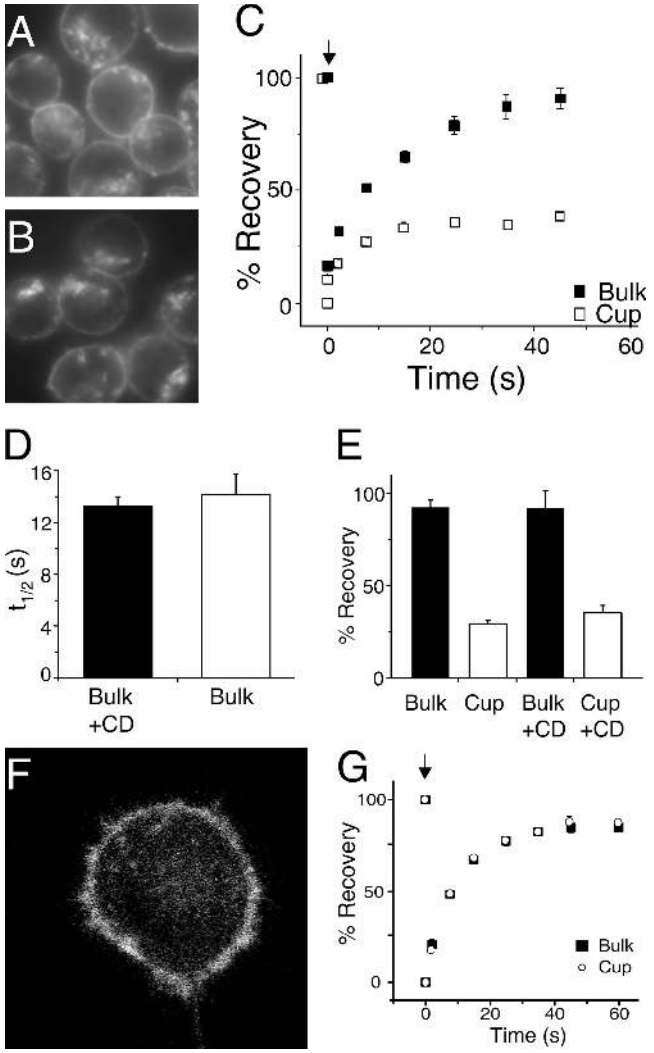

Figure 6. **Effect of cholesterol depletion on the mobility of PM-GFP.** (A and B) Effect of MβCD on cholesterol content. RAW264.7 cells were incubated in the presence (B) or absence (A) of 10 mM MβCD for 30 min, and their cholesterol content was observed by fluorescence microscopy after staining with filipin. (C) RAW264.7 cells transfected with PM-GFP were treated with or without MβCD as in A and B and then exposed to IgG-opsonized beads to initiate phagocytosis. The course of FRAP of PM-GFP is illustrated. Two areas were bleached: one near the middle of the cup (open squares) and the other in an unengaged area of the cell membrane (closed squares). (D) Comparison of the half-time for recovery of PM-GFP after bleaching in otherwise untreated (open bar) and in MβCD-extracted cells (solid bar). (E) Comparison of the fractional recovery of PM-GFP after bleaching at the phagocytic cup (open bars) and in unengaged regions of the membrane (solid bars) in cells undergoing phagocytosis. The cells had been either untreated or extracted with MβCD as specified. Data in D and E are means ± SEM of seven determinations. (F) LSM transverse optical slice acquired before bleaching of RAW cells transfected LAT-GFP. (G) Course of FRAP after bleaching at the phagocytic cup (open symbols) and in unengaged regions of the membrane (closed symbols) in cells undergoing the phagocytosis of 8.3-μm beads. Bleaching occurred at the arrow, and data are means ± SEM of six experiments of each type. Where absent, error bars were smaller than the symbol.

particularly in the case of large beads such as those used in this study (Fig. S3, C and F). As expected, LY294002 had no discernible effect on the mobility of the exofacial marker GPI-YFP. Interestingly, the immobilization of PM-GFP normally seen in untreated cells persisted in the presence of the inhibitor (MF = 0.46), as illustrated in Fig. 7 and quantified in Table I. These findings imply that generation of 3′-phosphorylated inositides is not essential to retain acylated molecules in the inner aspect of the phagocytic cup.

Discussion

Suitability of the probes used

The objective of our experiments was to assess the mobility of lipid-associated proteins in the phagosome and to define its determinants. The fluorescent proteins used in this study, such as PM-GFP and GFP-tH, are suitable probes to measure the contribution of the hydrophobic moiety of lipid-anchored molecules such as diacylated Src-family kinases and small GTPases, which are critical for the onset and development of phagocytosis. The molecular weight, acyl chain composition, and membrane disposition of the probes is very similar to that of the endogenous signaling molecules, yet they greatly simplify the analysis by obviating protein–protein interactions. In addition, acylated fluorescent proteins are arguably good models to analyze the mobility of lipids in the plane of the bilayer. At first glance, it may appear that attachment of the comparatively large protein moiety to the acyl chains would greatly reduce the lateral mobility of the complex, compared with that of endogenous phospholipids. However, hydrophobic interactions within the bilayer appear to be, by far, the main impediment to the lateral displacement of lipids and lipid-anchored proteins. We calculated diffusion coefficients of $\sim 2.3 \times 10^{-10}$ cm^2/s for labeled phospholipids and 1.5×10^{-10} cm^2/s for diacylated GFP in RAW cells. Such coefficients are nearly three orders of magnitude lower than that reported for GFP in water (9×10^{-7} cm^2/s), which is reduced only three- to fourfold when the protein is expressed in intracellular compartments, including the cytosol (Partikian et al., 1998; Chen et al., 2002). Therefore, attachment of a GFP moiety would be expected to contribute minimally to the mobility of the acyl chains in the plane of the membrane.

Reduced mobility of lipid-associated proteins at the phagocytic cup

The main observation reported in this paper is that the mobility of lipid-attached probes differs in the phagocytic cup from that in the bulk of the unengaged membrane. We considered whether fission of endocytic vesicles, too small to be detected by the optical microscope, accounted for the failure of the fluorescence to recover at the cup. Indeed, remodeling of the cup formed during ingestion of large beads commenced before sealing (Fig. S2). To minimize the confounding effect of this remodeling, all our experiments were performed at the onset of phagocytosis and limited to the first 100 s after bead engagement. More important, although all the lipids analyzed underwent parallel remodeling (Fig. S2), only PM-GFP and GFP-tH displayed reduced mobility. GPI-anchored probes, which are remodeled at a similar rate, recovered to a much greater extent, as did GFP-tK. Jointly, these considerations rule out endocytosis as a viable explanation for the incomplete fluorescence recovery.

The differential behavior of GPI-YFP, a probe located on the outer monolayer of the plasmalemma, and PM-GFP,

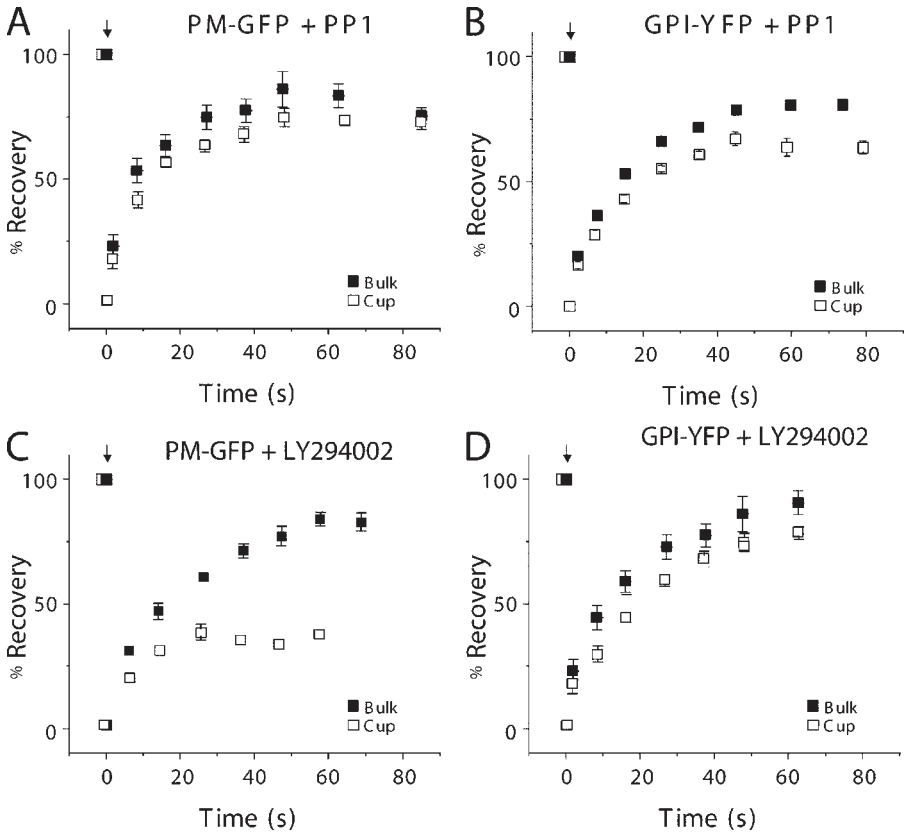

Figure 7. **Effect of kinase inhibitors on the mobility of inner and outer membrane leaflet probes.** RAW cells transfected with PM-GFP (A and C) or GPI-GFP (B and D) were pretreated with either 10 μM PP1 for 1 h (A and B) or 100 μM LY294002 for 30 min (C and D) and then exposed to 8.3-μm IgG-opsonized beads to initiate phagocytosis. PP1 or LY294002 were maintained in the medium during phagocytosis. The course of FRAP is illustrated. Two areas were bleached: one near the middle of the cup (open squares) and the other in an unengaged area of the cell membrane (closed squares). Data are means ± SEM of eight determinations. Where absent, error bars were smaller than the symbol.

an inner monolayer probe, could be attributed to a unique steric hindrance on the cytosolic face of the membrane. The actin cytoskeleton would be an obvious candidate for such a physical obstacle. Cytoskeletal proteins may restrict the motion of the GFP moiety and in extreme cases, corral it within domains that are fenced in. Several lines of evidence argue against this. First, although actin and its associated proteins do indeed accumulate at the base of the cup during the initial stages of phagocytosis, they subsequently detach (Video 1). In fact, in the case of large beads such as those used in our experiments, the density of actin below the forming phagosome drops below the levels of the unengaged membrane, where the mobility of the lipid-associated probe remains high. Moreover, lipid immobilization persisted in the region subtending the particle in cells treated with cytochalasin D to preclude actin polymerization. Moreover, in the absence of the inhibitor, an extreme situation is reached after the phagosome seals, when actin is no longer detectable on its membrane, yet the reduction in lipid mobility persisted (Fig. 4). Second, the mobility of GFP-tK was altered much less than that of GFP-tH or PM-GFP (Table I). Because the size and disposition of the protein moiety of the probes with respect to the membrane are similar in all cases, fencing in by cytoskeletal elements is an unlikely explanation for the altered mobility. Still, a contribution of the actin network to the mobility of the probes cannot be entirely ruled out. If it exists, such a steric hindrance would contribute little to the mobility of free lipids but would nevertheless affect lipid-associated proteins, whether the association is covalent, as in the case of Src-family kinases, or electrostatic, as in the case of proteins bearing PH domains.

We believe that immobilization of lipid microdomains in the vicinity of clustered Fcγ receptors is the most likely explanation for our observations. Lipid rafts, cholesterol-rich microdomains that also contain glycosphingolipids, are often invoked in the context of signal transduction by immunoreceptors (Magee et al., 2002). Both PM-GFP and GFP-tH would be expected to partition into such rafts, and coalescence of the latter around activated receptors may have contributed to immobilization of the probes. However, our observations do not fit the conventional model of the raft on two accounts. First, the mobility of GPI-YFP, which is predicted to reside in rafts, was similar in the cup and elsewhere in the membrane. Second, extraction of 50% of the total cellular cholesterol and likely an even greater fraction of the plasmalemmal cholesterol had little effect on the immobilization of PM-GFP at the cup. Two explanations can be considered: (1) that coalescence of lipid microdomains is not the mechanism underlying the change in lipid mobility and (2) that unique microdomains that do not conform to the conventional sphingolipid and cholesterol-rich raft are responsible. In this regard, it is noteworthy that unlike the situation reported for immunoreceptors in lymphoid and basophilic cells (Vereb et al., 2000; Surviladze et al., 2001), extraction of cholesterol does not impair Fcγ receptor signaling, leading to phagocytosis (Gatfield and Pieters, 2000; Peyron et al., 2000).

Passive coalescence of lipid microdomains cannot explain the sensitivity of the immobilization to inhibitors of Src-family kinases, which provide the earliest signal in the phagocytic cascade. We propose that events that follow tyrosine phosphorylation contribute to the assembly of lipid microdomains. It is

conceivable that the recruitment of adaptor molecules with lipid-interacting moieties facilitates the coalescence of specific lipids, thereby reducing their mobility. Two types of adaptors could fulfill this function by different mechanisms. Transmembrane molecules that preferentially associate with saturated lipids such as LAT can be recruited to activated receptor complexes (Ragab et al., 2003). The lipid annulus associated with LAT or similar adaptors could interact with and reduce the mobility of lipids with saturated chains in the immediate vicinity of the activated receptor complex. Of note, the mobility of LAT itself has been documented to be reduced when T cell receptors are stimulated (Tanimura et al., 2003). However, LAT is not an essential adaptor of Fc receptors in phagocytes, which use other adaptors such as Gab2, Grb2, and CrkII. Accordingly, we found that LAT is not recruited or immobilized at sites of phagocytosis. Other, unidentified transmembrane adaptors may nevertheless cause the immobilization of selected lipids near the activated receptors, but soluble adaptors could similarly be involved. Adaptors bearing lipid binding domains would be recruited to the receptor complex by the former and would stabilize lipids in its vicinity. Several adaptors possessing PH, ENTH (epsin N-terminal homology), or VHS (Vps27, Hrs, and Stam) domains are known to exist, and some of these, such as Gab2, have been reported to associate with Fcγ receptors (Gu et al., 2003). Some signaling molecules, such as Vav or PLCγ, become part of the activated receptor complex and contain lipid binding PH domains. Together, the proteins that cluster around activated receptors can cause immobilization of defined lipids. Importantly, the acyl moieties of phosphoinositides would facilitate accumulation and immobilization of other lipids with saturated chains and of proteins like diacylated Src-family kinases or GTPases.

In summary, we propose a model whereby clustering and activation of Fcγ receptors may lead to the recruitment and stabilization of specific lipids and/or lipid-associated proteins in the active zone. Adaptors or other signaling molecules that become recruited to the signaling complex may induce the formation of a defined lipid annulus, effectively a microdomain that need not be stabilized by cholesterol but by hydrophobic interactions between the saturated acyl chains of its constituents. Such stabilization would have critical consequences for localized signaling, restricting the diffusion of phosphoinositides and focally attracting adaptors and transducers.

Materials and methods

Reagents

Polystyrene beads (3.1 and 8.3 μm in diameter) were obtained from Bangs Laboratories. FuGene 6 was purchased from Roche Molecular Biochemicals. PP1 was obtained from BIOMOL Research Laboratories, Inc., LY294002 from Calbiochem, and α-MEM from Wisent, Inc. Cy3-labeled secondary antibodies were obtained from Jackson ImmunoResearch Laboratories. Rhodamine-phalloidin and the Amplex red cholesterol assay kit were obtained from Invitrogen. Human IgG, MβCD, filipin, and all other reagents were obtained from Sigma-Aldrich. The headgroup-labeled lipids nitrobenzoxadiazole (NBD)-phosphatidylserine and boron dipyrromethene difluoride (BODIPY)–phosphatidylethanolamine were purchased from Avanti Polar Lipids, Inc., and Invitrogen, respectively. The synthetic medium used for fluorescence determinations consisted of 140 mM NaCl, 3 mM KCl, 10 mM glucose, 20 mM Hepes, 1 mM $MgCl_2$, and 1 mM $CaCl_2$, pH 7.4 (290 ± 5 mosM).

cDNA constructs

PM-GFP encodes the 10 amino acid myristoylation/palmitoylation sequence from Lyn fused to enhanced GFP (Teruel et al., 1999). GFP-tH consists of the C-terminal 9 amino acids of H-Ras fused to the C terminus of GFP. GFP-tK consists of the C-terminal 17 amino acids of K-Ras fused to the C terminus of GFP. These C-terminal regions comprise the complete targeting domains of H- and K-Ras, respectively (Apolloni et al., 2000). GPI-GFP and -YFP encode the 26 amino acid signal sequence of insulin fused to enhanced GFP or YFP, followed by the 43 amino acid GPI sequence motif of decay-accelerating factor (Kenworthy et al., 2004). Construction of the LAT-GFP plasmid was detailed in Bonello et al. (2004). For localization of PtdIns(4,5)P_2 and PtdIns(3,4,5)P_3, we used enhanced GFP fusions of the PH domains of PLCδ or Akt, respectively, both gifts from T. Meyer (Stanford University, Stanford, CA).

Cell culture, transfection, and phagocytosis

The macrophage RAW264.7 cell line was obtained from American Type Culture Collection. These macrophages, referred to hereafter and throughout as RAW cells, were cultured in α-MEM supplemented with 10% fetal calf serum at 37°C under a humidified 5% CO_2 atmosphere. Cells were trypsinized and seeded onto 2.5-cm glass coverslips at ∼30% confluence. Cells were transiently transfected by lipofection using FuGene 6 or by electroporation with the Nucleofector system (Amaxa) according to the manufacturers' directions and used within 16–24 h of transfection. Polystyrene beads were opsonized with 1 mg/ml human IgG by incubation for at least 1 h at 37°C, followed by three washes with PBS. To initiate phagocytosis, opsonized beads were allowed to sediment on RAW cells grown on coverslips and bathed in synthetic medium at 37°C.

Loading of fluorescent lipids

RAW macrophages were grown on glass coverslips to ∼30% confluence. 50 μl of either lipid (dissolved in chloroform) were added to 9.5 ml of synthetic medium supplemented with 1 ml bovine serum albumin and mixed vigorously. Cells were overlaid with the lipid suspension and incubated at 4°C for 60 min. Cells were then washed and warmed with medium at 37°C before measuring fluorescence.

Fluorescence determinations

The distribution and mobility of the fluorescent chimeras was analyzed by confocal microscopy. Laser-scanning confocal microscopy was performed with a LSM510 system (Carl Zeiss MicroImaging, Inc.) using a 100× (1.4 NA) oil-immersion objective lens. The standard laser excitation line (488 nm) and emission filter (543 nm) were used to image GFP and YFP-tagged chimeras. Coverslips bearing transfected cells were transferred to a thermostatted Leiden chamber holder on the microscope stage, where they were maintained at 37°C.

For measurements of FRAP, two areas of 2 μm in diameter, one at the phagosomal cup and a second one at an unengaged portion of the plasmalemma of the same cell were defined. After acquiring three basal readings, the selected regions were irreversibly photobleached by repeated exposure to the 488-nm laser line set at 100% power. Under the conditions of our experiments (18 mW power output), nearly complete bleaching required 60 iterations, a process that was completed in 1–2 s. The recovery of fluorescence was then monitored over time by scanning the bleached area at the conventional (low) laser power to minimize photobleaching during sampling.

To determine the size and shape of the bleached area, cells were fixed with 4% paraformaldehyde for 1 h before mounting in the Leiden chamber, to prevent lateral mobility of the tagged proteins and recovery of fluorescence. Photobleaching was then performed as described in the previous paragraph, and fluorescence images were obtained throughout the height of the cell by optical sectioning using the confocal microscope. Three-dimensional reconstruction of the stacked images using the LSM510 software enabled us to reconstruct the pattern of the bleached area.

FRAP data analysis

To analyze the rate of recovery, we compared the fluorescence of the bleached area to that of an adjacent unbleached area of the same cell with similar fluorescence intensity. For each time point, the fluorescence of the bleached area was normalized to that of the corresponding control (unbleached) area to correct for possible drift of the focal plane or photobleaching incurred during the low-light sampling. For reference, images of the entire field were acquired immediately before and at the end of the experiment. All FRAP measurements were performed at 37°C. Data were

fit to a simple diffusion, zero flow model (Yguerabide et al., 1982) using the formula

$$F(t) = \frac{F_{(t=0)} + F_{(t=\infty)} \times (t/t_{1/2})}{1 + (t/t_{1/2})},$$

where the fluorescence intensity (F) at a given time (t) is related to the maximal fluorescence ($F_{(t=\infty)}$) and the half-time of maximal recovery ($t_{1/2}$). Using this equation, recovery curves were fit by least squares using Prism 4 (GraphPad Software, Inc.). In all cases, this method provided highly significant R^2 values that were comparable to and generally larger than those obtained using other models for single or multiple components of diffusion or flow (Yguerabide et al., 1982; Lippincott-Schwartz et al., 1999). Diffusion coefficients were calculated from the $t_{1/2}$ of the recovery curves as previously described (eq. 19 in Axelrod et al., 1976).

Actin staining and manipulation

To label F-actin, cells were washed twice with PBS and fixed with 4% paraformaldehyde for 1 h. The cells were next permeabilized in 0.1% Triton X-100 and 100 mM glycine in PBS for 10 min and stained with a 1:400 dilution of rhodamine-phalloidin for 1 h. Where specified, actin polymerization was impaired by pretreating the cells with 2 μM cytochalasin D for 10 min at 37°C as previously described (Greenberg et al. 1994). The inhibitor was maintained in the medium throughout the fluorescence determinations.

Cholesterol manipulation and determination

Where indicated, the cells were incubated with 10 mM MβCD for 30 min at 37°C to remove cholesterol. To verify the effectiveness of the treatment, cells were then fixed with 4% paraformaldehyde and incubated with 25 μg/ml of filipin, a cholesterol binding fluorescent probe, in PBS containing 1 mM $MgCl_2$ and $CaCl_2$ for 1 h at 4°C. Cells were then washed twice with PBS, and images were acquired with excitation at 488 nm and emission at 500–550 nm. More quantitative estimates of cholesterol content were made using the Amplex red cholesterol assay kit, according to the manufacturer's instructions.

Pharmacological inhibition of kinases

To inhibit phosphatidylinositol 3-kinases or Src-family kinases, RAW cells were exposed to either 100 μM LY294002 for 30 min or 10 μM PP1 for 1 h, respectively, at 37°C before the fluorescence determinations. Inhibitors were maintained in the medium throughout the microscopy experiments.

Online supplemental material

Fig. S1 provides an estimation of the time required for the phagocytic internalization of beads of different sizes by RAW macrophages. Fig. S2 shows the persistence of inner and outer leaflet membrane probes during phagocytosis. Fig. S3 shows the distribution of phospholipid probes for PtdIns(4,5)P_2 and PtdIns(3,4,5)P_3 in the presence of Src-family kinase and PI3K inhibitors during phagocytosis. Video 1 shows the transient remodeling of actin during the phagocytosis of an 8-μm bead. Online supplemental material is available at http://www.jcb.org/cgi/content/full/jcb.200605044/DC1.

We thank Dr. B. Grinstein (Department of Physics, University of California, San Diego, La Jolla, CA) for his invaluable help with curve-fitting models.

This work was supported by grants from the Canadian Institutes of Health Research (CIHR) and the Heart and Stroke Foundation of Canada. E.F. Corbett-Nelson was the recipient of a postdoctoral fellowship award from CIHR. S. Grinstein is the current holder of the Pitblado Chair in Cell Biology and was cross-appointed to the Department of Biochemistry at the University of Toronto.

Submitted: 5 May 2006
Accepted: 14 June 2006

References

Apolloni, A., I.A. Prior, M. Lindsay, R.G. Parton, and J.F. Hancock. 2000. H-ras but not K-ras traffics to the plasma membrane through the exocytic pathway. *Mol. Cell. Biol.* 20:2475–2487.

Araki, N., M.T. Johnson, and J.A. Swanson. 1996. A role for phosphoinositide 3-kinase in the completion of macropinocytosis and phagocytosis by macrophages. *J. Cell Biol.* 135:1249–1260.

Axelrod, D., D.E. Koppel, J. Schlessinger, E. Elson, and W.W. Webb. 1976. Mobility measurement by analysis of fluorescence photobleaching recovery kinetics. *Biophys. J.* 16:1055–1069.

Azzoni, L., M. Kamoun, T.W. Salcedo, P. Kanakaraj, and B. Perussia. 1992. Stimulation of FcγRIIIA results in phospholipase C-γ1 tyrosine phosphorylation and p56lck activation. *J. Exp. Med.* 176:1745–1750.

Bonello, G., N. Blanchard, M.C. Montoya, E. Aguado, C. Langlet, H.T. He, S. Nunez-Cruz, M. Malissen, F. Sanchez-Madrid, D. Olive, et al. 2004. Dynamic recruitment of the adaptor protein LAT: LAT exists in two distinct intracellular pools and controls its own recruitment. *J. Cell Sci.* 117:1009–1016.

Botelho, R.J., M. Teruel, R. Dierckman, R. Anderson, A. Wells, J.D. York, T. Meyer, and S. Grinstein. 2000. Localized biphasic changes in phosphatidylinositol-4,5-bisphosphate at sites of phagocytosis. *J. Cell Biol.* 151:1353–1368.

Chen, Y., J.D. Muller, Q. Ruan, and E. Gratton. 2002. Molecular brightness characterization of EGFP in vivo by fluorescence fluctuation spectroscopy. *Biophys. J.* 82:133–144.

Cox, D., C.C. Tseng, G. Bjekic, and S. Greenberg. 1999. A requirement for phosphatidylinositol 3-kinase in pseudopod extension. *J. Biol. Chem.* 274:1240–1247.

Fadok, V.A., D.R. Voelker, P.A. Campbell, J.J. Cohen, D.L. Bratton, and P.M. Henson. 1992. Exposure of phosphatidylserine on the surface of apoptotic lymphocytes triggers specific recognition and removal by macrophages. *J. Immunol.* 148:2207–2216.

Galbiati, F., B. Razani, and M.P. Lisanti. 2001. Emerging themes in lipid rafts and caveolae. *Cell.* 106:403–411.

Gatfield, J., and J. Pieters. 2000. Essential role for cholesterol in entry of mycobacteria into macrophages. *Science.* 288:1647–1650.

Greenberg, S., P. Chang, and S.C. Silverstein. 1994. Tyrosine phosphorylation of the γ subunit of FCγ receptors, $p72^{syk}$, and paxillin during Fc receptor-mediated phagocytosis in macrophages. *J. Biol. Chem.* 269:3897–3902.

Gu, H., R.J. Botelho, M. Yu, S. Grinstein, and B.G. Neel. 2003. Critical role for scaffolding adapter Gab2 in FcγR-mediated phagocytosis. *J. Cell Biol.* 161:1151–1161.

Hinchliffe, K.A., A. Ciruela, and R.F. Irvine. 1998. PIPkins1, their substrates and their products: new functions for old enzymes. *Biochim. Biophys. Acta.* 1436:87–104.

Kenworthy, A.K., B.J. Nichols, C.L. Remmert, G.M. Hendrix, M. Kumar, J. Zimmerberg, and J. Lippincott-Schwartz. 2004. Dynamics of putative raft-associated proteins at the cell surface. *J. Cell Biol.* 165:735–746.

Klein, U., G. Gimpl, and F. Fahrenholz. 1995. Alteration of the myometrial plasma membrane cholesterol content with beta-cyclodextrin modulates the binding affinity of the oxytocin receptor. *Biochemistry.* 34:13784–13793.

Kusumi, A., I. Koyama-Honda, and K. Suzuki. 2004. Molecular dynamics and interactions for creation of stimulation-induced stabilized rafts from small unstable steady-state rafts. *Traffic.* 5:213–230.

Kwiatkowska, K., and A. Sobota. 2001. The clustered Fcgamma receptor II is recruited to Lyn-containing membrane domains and undergoes phosphorylation in a cholesterol-dependent manner. *Eur. J. Immunol.* 31:989–998.

Kwiatkowska, K., J. Frey, and A. Sobota. 2003. Phosphorylation of FcgammaRIIA is required for the receptor-induced actin rearrangement and capping: the role of membrane rafts. *J. Cell Sci.* 116:537–550.

Liao, F., H.S. Shin, and S.G. Rhee. 1992. Tyrosine phosphorylation of phospholipase C-gamma 1 induced by cross-linking of the high-affinity or low-affinity Fc receptor for IgG in U937 cells. *Proc. Natl. Acad. Sci. USA.* 89:3659–3663.

Lippincott-Schwartz, J., J.F. Presley, K.J.N. Zaal, K. Hirschberg, C.D. Miller, and J. Ellenberg. 1999. Monitoring the dynamics and mobility of membrane proteins tagged with GFP. *Methods Cell Biol.* 58:261–281.

Magee, T., N. Pirinen, J. Adler, S.N. Pagakis, and I. Parmryd. 2002. Lipid rafts: cell surface platforms for T cell signaling. *Biol. Res.* 35:127–131.

Majeed, M., E. Caveggion, C.A. Lowell, and G. Berton. 2001. Role of Src kinases and Syk in Fcgamma receptor-mediated phagocytosis and phagosome-lysosome fusion. *J. Leukoc. Biol.* 70:801–811.

Marshall, J.G., J.W. Booth, V. Stambolic, T. Mak, T. Balla, A.D. Schreiber, T. Meyer, and S. Grinstein. 2001. Restricted accumulation of phosphatidylinositol 3-kinase products in a plasmalemmal subdomain during Fcγ receptor-mediated phagocytosis. *J. Cell Biol.* 153:1369–1380.

Nichols, B.J. 2003. GM1-containing lipid rafts are depleted within clathrin-coated pits. *Curr. Biol.* 13:686–690.

Oancea, E., M.N. Teruel, A.F. Quest, and T. Meyer. 1998. Green fluorescent protein (GFP)-tagged cysteine-rich domains from protein kinase C as fluorescent indicators for diacylglycerol signaling in living cells. *J. Cell Biol.* 140:485–498.

Partikian, A., B. Olveczky, R. Swaminathan, Y. Li, and A.S. Verkman. 1998. Rapid diffusion of green fluorescent protein in the mitochondrial matrix. *J. Cell Biol.* 140:821–829.

Peyron, P., C. Bordier, E.N. N'Diaye, and I. Maridonneau-Parini. 2000. Nonopsonic phagocytosis of *Mycobacterium kansasii* by human neutrophils depends on cholesterol and is mediated by CR3 associated with glycosylphosphatidylinositol-anchored proteins. *J. Immunol.* 165:5186–5191.

Ragab, A., S. Bodin, C. Viala, H. Chap, B. Payrastre, and J. Ragab-Thomas. 2003. The tyrosine phosphatase 1B regulates linker for activation of T-cell phosphorylation and platelet aggregation upon FcgammaRIIa cross-linking. *J. Biol. Chem.* 278:40923–40932.

Simons, K., and E. Ikonen. 1997. Functional rafts in cell membranes. *Nature.* 387:569–572.

Song, X., S. Tanaka, D. Cox, and S.C. Lee. 2004. Fcgamma receptor signaling in primary human microglia: differential roles of PI-3K and Ras/ERK MAPK pathways in phagocytosis and chemokine induction. *J. Leukoc. Biol.* 75:1147–1155.

Stauffer, T.P., and T. Meyer. 1997. Compartmentalized IgE receptor-mediated signal transduction in living cells. *J. Cell Biol.* 139:1447–1454.

Surviladze, Z., L. Draberova, M. Kovarova, M. Boubelik, and P. Draber. 2001. Differential sensitivity to acute cholesterol lowering of activation mediated via the high-affinity IgE receptor and Thy-1 glycoprotein. *Eur. J. Immunol.* 31:1–10.

Swaminathan, R., S. Bicknese, N. Periasamy, and A.S. Verkman. 1996. Cytoplasmic viscosity near the cell plasma membrane: translational diffusion of a small fluorescent solute measured by total internal reflection-fluorescence photobleaching recovery. *Biophys. J.* 71:1140–1151.

Tanimura, N., M. Nagafuku, Y. Minaki, Y. Umeda, F. Hayashi, J. Sakakura, A. Kato, D.R. Liddicoat, M. Ogata, T. Hamaoka, and A. Kosugi. 2003. Dynamic changes in the mobility of LAT in aggregated lipid rafts upon T cell activation. *J. Cell Biol.* 160:125–135.

Teruel, M.N., T.A. Blanpied, K. Shen, G.J. Augustine, and T. Meyer. 1999. A versatile microporation technique for the transfection of cultured CNS neurons. *J. Neurosci. Methods.* 93:37–48.

Tse, S.M., W. Furuya, E. Gold, A.D. Schreiber, K. Sandvig, R.D. Inman, and S. Grinstein. 2003. Differential role of actin, clathrin, and dynamin in Fc gamma receptor-mediated endocytosis and phagocytosis. *J. Biol. Chem.* 278:3331–3338.

Varnai, P., K.I. Rother, and T. Balla. 1999. Phosphatidylinositol 3-kinase-dependent membrane association of the Bruton's tyrosine kinase pleckstrin homology domain visualized in single living cells. *J. Biol. Chem.* 274:10983–10989.

Vereb, G., J. Matko, G. Vamosi, S.M. Ibrahim, E. Magyar, S. Varga, J. Szollosi, A. Jenei, R. Gaspar Jr., T.A. Waldmann, and S. Damjanovich. 2000. Cholesterol-dependent clustering of IL-2Ralpha and its colocalization with HLA and CD48 on T lymphoma cells suggest their functional association with lipid rafts. *Proc. Natl. Acad. Sci. USA.* 97:6013–6018.

Vieira, O.V., R.J. Botelho, and S. Grinstein. 2002. Phagosome maturation: aging gracefully. *Biochem. J.* 366:689–704.

Yguerabide, J., J.A. Schmidt, and E.E. Yguerabide. 1982. Lateral mobility in membranes as detected by fluorescence recovery after photobleaching. *Biophys. J.* 40:69–75.